TOUGHNESS AND GROWTH OF FATIGUE CRACKS IN PM STEELS

J. R. Moon

Abstract

At relative densities of ρ_r~0.9, strength and toughness depend on the fraction of overall volume that is deformed; this scales with (neck diameter/particle diameter)^n where n is between 3 and 4. At ρ_r~1.0, good fracture toughnesses, K_Q, and fractures formed by microvoid coalescence go with low strength microstructures, whereas cleavage and poor toughness is concomitant of high strength. Paris exponents for steady state crack growth are governed by fracture toughness in the same way as wrought steels. They are high when ρ_r~0.9; cracks extend by rupturing sinter necks or through particles. When ρr~1.0, exponents are between 2.6 and 4.0, typical of wrought steels. Cracks grow partly by true fatigue modes and partly by bursts of cleavage, depending on how closely K_{MAX} approaches K_Q.

Keywords: PM steels, homogeneously alloyed, heterogeneously alloyed, interconnected pore regime, disconnected pore regime, fracture toughness, fatigue crack growth

INTRODUCTION

The increasing range of present and potential applications of PM steels provides a continuing incentive for improvement of mechanical properties in general. Requirements include abilities to withstand heavy loads, both statically and dynamically. For many applications, fatigue performance is crucial [1, 2]. There are two interconnected and interwoven approaches available to the PM community. To satisfy the demands of designers, we must provide design data for materials that are expected to remain available over a long time-scale [3, 4]. We must also be looking to develop better materials, which implies a development of scientific understanding of the micro-mechanisms of fracture.

As always, the starting point is to look at the behaviour of wrought steels. S – N curves established in both rotating bending and alternating axial modes exhibit endurance limits at stress amplitudes that are usually at about 40% of the ultimate tensile strength of the material [5]. The same was thought to be true for PM steels [6-8], although it now appears that there is a decline in performance at very large numbers of cycles [9].

Improvements in endurance limits follow improvements in strength. The main way of achieving this is by reducing the total porosity [10], or perhaps it is just necessary to reduce the number of large pores [11]. Debate centres around whether this is done best by warm compaction, high temperature sintering, powder forging or by any other means.

Many bulk properties, electrical and thermal conductivities [12, 13] elastic moduli [14], strengths, ductilities and toughnesses [15-17] are influenced by the volume fraction of pores and by details of their shapes. The influence of the pores is much more profound than would be expected simply from the loss of volume or cross-sectional area of metal in the

John Robert Moon, School of Mechanical, Materials, Manufacturing Engineering and Management, University of Nottingham, Nottingham, United Kingdom

material. At volume fractions of pores greater than ~10%, the pores are mostly interconnected. The load bearing path through the material goes through the inter-particle necks. Much depends on the fraction of the material represented by these necks and the local properties of the material within them [18-21]. When the porosity is decreased to less than ~8%, the pores become disconnected from one another and surrounded completely by metallic matrix. The load bearing path through the matrix is disturbed by the pores and much now depends on the stress concentrations arising at their edges. In turn these are functions of the pore shapes, sizes and the distances between them. Inclusions in the material also play a role, particularly when the porosity approaches zero, as with powder forgings [22-24].

Further improvements come from alloying. Here, distinction is required between fully pre-alloyed powders that give rise to homogeneous microstructures and diffusion alloyed materials. Microstructures that have been formed by diffusion alloying during sintering can in principle contain every equilibrium phase and phase mixture and all the metastable transformation products described in the textbooks on steel metallurgy. Their relative quantities and distributions are affected critically by details of processing such as particle volumes and surface areas, sintering temperatures and times, heat-treatment details and so forth. It is not surprising that all the variations and their interactions have not been studied and that questions about which is the best type of microstructure remain a continuing topic of debate [25-29].

Failure in monotonic loading as well as in fatigue is along the path of least resistance. But, is this through a small neck whose toughness is enhanced by the presence of retained austenite or through a bulkier neck containing less tough pearlite or high carbon martensite? Analogies with wrought steels would lead us to suppose that, within a coherent family of alloys, toughness, as measured by impact testing or as plane strain fracture toughness, would decline as yield strength was increased [30, 31]. But, for PM materials with porosities within the interconnected range, both toughness and yield strength increase when either the sizes of inter-particle necks are increased or their local strengths are increased by alloying[15-21].

Inclusions, or rather their absence, are important [22-24, 29]. Not only are they initiators of fatigue cracks, but also they can provide paths of rapid crack advance or, in rare cases, stop a crack from progressing. The inclusions may not be obvious. For example, non-adherence of contacting particle surfaces has been attributed to a remnant oxide film on the surfaces, even after sintering in oxide reducing atmospheres [36]. An advancing crack finding such a feature would be expected to take advantage and propagate rapidly along it. Certainly, it has been found that S-N endurance limits were enhanced by reducing the oxygen content of the material [36]; the best way was by starting with a clean powder.

Measurements of plane strain fracture toughness, K_{IC}, are tricky to carry out and awkward to interpret. The problem is that test-pieces must contain completely the plastic zone associated with and running ahead of an advancing crack. The size of this plastic zone is ~ $(K_{IC}/\sigma_y)^2/6\pi$ and when yield stresses are low we need very large test-pieces in order to carry out valid tests. Most data quoted for K_{IC} of PM materials do not satisfy this validity criterion and so cannot be taken as absolute measurements [37]. Instead, they are sometimes quoted as K_Q and represent the best that we can do at the moment. Nevertheless, the data has some value as a guide to understanding micro-mechanisms. A comprehensive collection has been made of data existing prior to the year 2000 [38]. It seems to confirm the ideas that inter-particle neck sizes and strengths are important in the range of interconnected pores, but that when the pores are disconnected, the properties of the matrix are the dominant factor [37-40].

Application of the fracture mechanics approach to fatigue crack growth is somewhat easier. The plastic zone size at the crack tip is smaller, $\sim(K_{max}/\sigma_y)^2/6\pi$, where now K_{max} is the stress intensity developed at the crack tip when the load is at the maximum for the cycle. Since $K_{max} < K_{IC}$, often substantially so, this means that small test-pieces can be used validly [41-45].

The general patterns of behaviour for PM materials have been shown to mirror those of wrought materials [40-44]. Rates of crack growth, da/dN, depend on the range of applied stress intensity, ΔK. At intermediate values of ΔK, the crack growth rate follows the Paris law, $da/dn = C(\Delta K)^m$; at high values of ΔK, the crack growth rates accelerate toward the final catastrophic failure; at low values of ΔK there is a threshold value of ΔK below which crack growth cannot be discerned.

When ΔK is within the Paris regime, reducing the porosity of the material gives a general reduction in da/dN and, more importantly, a reduction in the Paris exponent, m. This is true throughout the porosity range but is more pronounced when the pores are disconnected. Threshold stress intensities are more complicated matter. These seem to increase as the porosity is reduced in the interconnected range, ie $\rho_r < 0.9$, but to remain constant at lower porosities, or even reduce a little as the porosity approaches zero. Generally, homogeneous powders give slightly better performance than inhomogeneous materials; thresholds are higher and growth exponents lower. For diffusion alloyed materials, high temperature sintering, which allows more extensive diffusion and less heterogeneous microstructures, gives generally higher thresholds and lower growth exponents.

MATERIALS STUDIED, PROCESSING AND MICROSTRUCTURES

All materials considered here are based on the well known Höganäs powders ASC100.29 (Fe), Astaloy A and Distaloy AB. After blending with graphite, these were processed as indicated in Tab.1.

Some material was examined as sintered; some after heat - treatment. Before heat-treatment, test - pieces were roughed out to oversize. After heat - treatment, all test - pieces were finished to size by grinding.

Tab.1. Materials, processing and products.

Materials Fe (ASC 100.29) - 0.5%C Distaloy AB (1.75Ni, 0.5Mo, 1.5Cu) - 0.6%C Astaloy A (1.9Ni, 0.5Mo, 0.25Mn, 0.08Cr) - 0.2 & 0.6%C
Pressed & sintered materials Blended with graphite & Pressed in carbide dies Sintered in Endogas (74% H_2, 25% N_2, 1% CH_4), 30 minutes at 1150°C Discs, 80 mm diameter, 50 mm thick, ρ_r~0.90
Rotary compacted & sintered Blended with graphite & Rotary compacted to ρ_r~0.95 Sintered in Endogas (74% H_2, 25% N_2, 1% CH_4), 30 minutes at 1120°C, 1250°C or 1350°C Rings, 60 mm/16 mm outer/inner diameters, 11 mm thick, ρ_r~0.95
Powder forgings Pressed & sintered to ρ_r~0.9 Hot - repressing at 1200°C Discs, 80mm diameter, 50mm thick, ρ_r~1.0 Bars, 120mm x 30mm x 20mm, ρ_r~1.0 (20mm parallel to pressing direction)
Heat – treatment Austenitised, 60 minutes at 850°C Quenched into "Iloquench" oil at 40°C (using sealed quench unit) Tempered in air circulating oven

MEASUREMENTS

Density was assessed from masses and physical dimensions of regular shaped pieces produced at intermediate stages in the preparation of test - pieces.

Tensile properties were measured using double shouldered test - pieces, cut from the originally formed blanks such that the testing direction was perpendicular to the original pressing direction.

Fracture toughness was assessed in mode 1 crack opening. This was done either by using symmetrical three - point bending, according to BS 5447:1977 or by pulling on the ends of half-ring test - pieces designed according to [47]. The half-ring geometry was used for rotary compacted and sintered materials; the process dictates the range of shapes that can be made and consequently the types of test - pieces that can be extracted from them [46]. Crack initiating slots were made by spark erosion and pre - cracks were grown by fatigue to a depth such that $0.45 < a/W < 0.55$. Final fracture was generated in both cases using machine cross - head displacements of 2mm/minute; crack opening displacement was measured using a clip gauge.

Measurements of fatigue crack propagation rates were made using the same forms of test - piece as for fracture toughness. Loads were oscillated in sine wave mode at 50Hz. Crack depth was monitored continuously using a DC potential drop method. A current of ~10A was passed along the length of the test-piece and the potential drops between points straddling the crack were monitored. Crack depths were assessed from independently derived calibrations.

Tests were conducted at constant stress ratios of either 0.1 or 0.8. Cracks were propagated using a load shedding routine from an initial $\Delta K \sim 20$ MPa$\sqrt{m}$. At each load reduction, the crack was allowed to grow beyond the plastic zone formed at the previous loading before its new growth rate was assessed. Plastic zones were estimated by conventional calculations assuming plane strain conditions and a homogeneous material.

Data for fracture toughness, K_Q

The first point to be noted is that no tests satisfied the validity criterion for fracture toughness testing and so results are quoted as K_Q, not K_{IC}. They must be taken only as indications of the relative toughnesses of the materials when tested in the ways they were! The data are plotted against density and 0.2% proof stress in Fig.1 and 2; these Figures include data taken from the collection made by Dudrova et al [38].

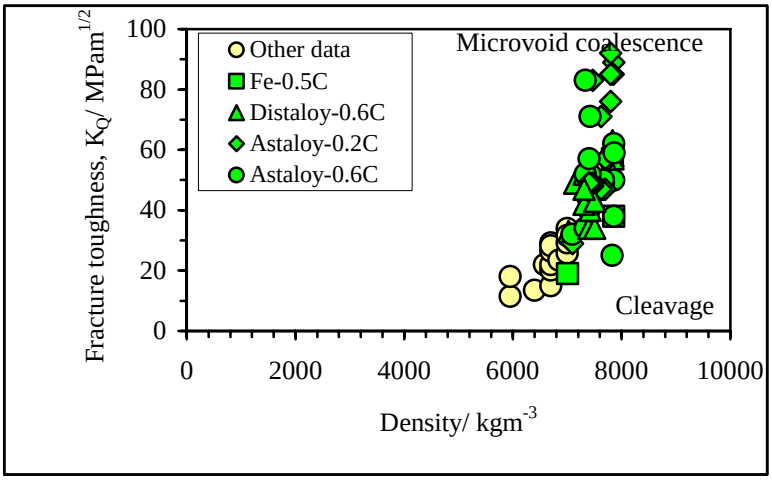

Fig.1. Relationship between fracture toughness K_Q and density.

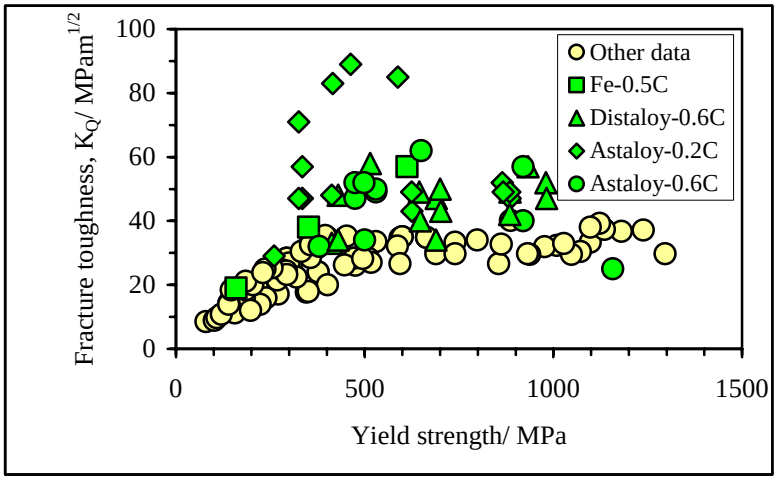

Fig.2. Relationship between fracture toughness, K_Q and yield strength.

As long as σ_y <500 MPa, toughness increases as yield strength increases, in accordance with the behaviour of most non-metallic materials [31]. Generally this behaviour is associated with relatively high porosities, >10%. At densities greater than ~92-95%, we have higher strengths and K_Q diminishes as σ_y increases, in accord with the behaviour expected of wrought steels [30,31]. In both regimes, toughnesses are higher when the carbon content is low. Differences between homogeneously alloyed and heterogeneously alloyed materials are hard to detect, but there is a weak suggestion that inhomogeneous Distaloy is better than homgeneous Astaloy at the same carbon content.

Figure 3 shows a plot against density of the quantity $(K_Q/\sigma_y)2/6\pi$, which gives us the approximate extent of the plastic zone associated with the crack tip under plane strain conditions when $K = K_Q$ (the plane stress zone is three times as large). Most results fall within a broad band, but those for low carbon Astaloy emphasise the good fracture toughness of this material.

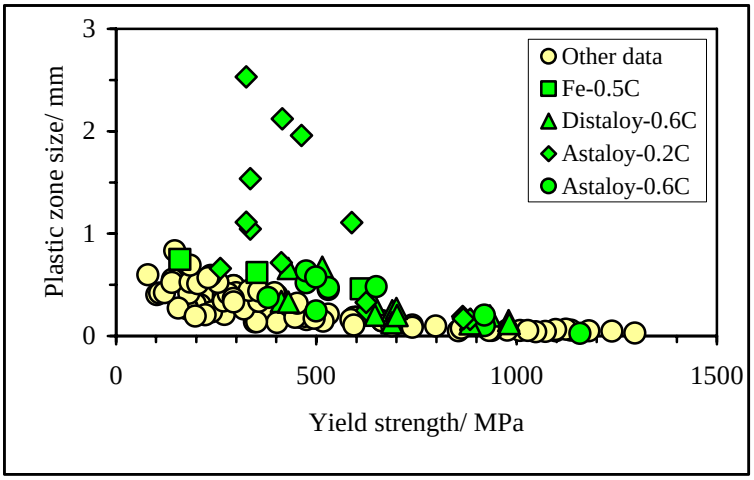

Fig.3. The sizes of the plastic zone at the crack tip as a function of yield stress; Plastic zone size is calculated as $\delta \sim (K_Q/\sigma_y)2/6\pi$.

Monotonic fracture surfaces

Table 2 summarises. Fractures of low density materials proceed by successive rupture of inter-particle necks. Nearly always these ruptures are by coalescence of microvoids formed during the local plastic deformation that precedes fracture. An example is in Fig.4.

At high densities, fracture may be totally by microvoid coalescence, totally by cleavage, or by a mixture of the two modes; examples are in Fig.5, 6 and 7.

Tab.2. Summary of Monotonic Fracture Surfaces.

Material	Pressed & Sintered (r_r~0.9)		Powder Forged (r_r~0.99)	
	as - formed	heat - treated	as - formed	heat - treated
Iron 0.6%C	ductile neck fractures by MVC, large areas of unbonded particles	ductile neck fractures by MVC, large areas of unbonded particles	100% cleavage	10 - 20% ductile 80 - 90% cleavage
Astaloy 0.2%C	ductile neck fractures by MVC, large areas of unbonded particles	ductile neck fractures by MVC, large areas of unbonded particles	100% ductile fracture by MVC	100% ductile fracture by MVC
Astaloy 0.6%C	ductile neck fractures by MVC, large areas of unbonded particles	ductile neck fractures by MVC, large areas of unbonded particles	100% cleavage	100% cleavage
Distaloy 0.6%C	ductile neck fractures by MVC, large areas of unbonded particles	ductile neck fractures by MVC, large areas of unbonded particles	~ 50% ductile MVC ~ 50% cleavage	~ 50% ductile MVC ~ 50% cleavage
MVC : microvoid coalescence River markings on cleaved surfaces point to weakness in a or to cracked inclusion, etc.				

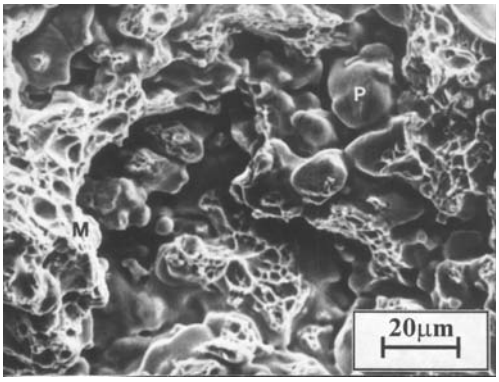

Fig.4. Characteristic monotonic fracture surface of pressed and sintered materials at relative densities, ρ_r, ~ 0.9. Fracture is by microvoid coalescence in sinter necks; in this case ~35% of the overall area is occupied by local fractures. This sample is Astaloy A – 0.2% C, as sintered, K_Q = 30 MPa$\sqrt{m}$.

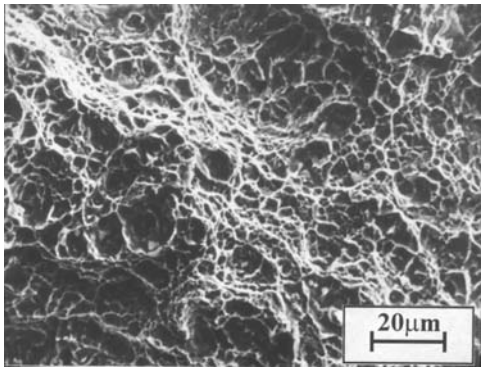

Fig.5. Monotonic fracture surface of powder forged Astaloy A – 0.2% C, ρ_r = 0.99. The whole area is formed by microvoid coalescence, K_Q = 90 MPa√m.

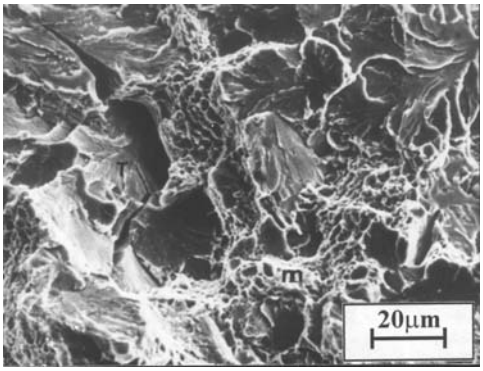

Fig.6. Monotonic fracture surface of powder forged Distaloy A – 0.6% C. ρ_r = 0.99. It shows a mixture of areas formed by microvoid coalescence and by cleavage, K_Q = 58 MPa√m.

High toughnesses correlate with microvoid coalescence (MVC); this was the only mode found for low carbon Astaloy. Low toughnesses correlate with extensive cleavage; this was the only mode for high carbon Astaloy after heat-treatment. Mixed mode fracture surfaces are most common; the correlation of K_Q with the fraction of MVC shown in Fig.8 is beguiling, but has to be treated with caution, noting the large errors and the small number of data points. The heterogeneously alloyed Distaloy always gave mixed mode fractures, mostly around 40-60% of microvoid coalescence.

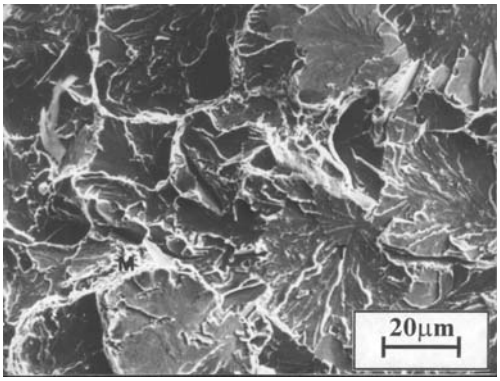

Fig.7. Monotonic fracture surface of powder forged Astaloy A – 0.6% C. ρ_r = 0.99. The fracture is nearly all by cleavage, K_Q = 30 MPa√m.

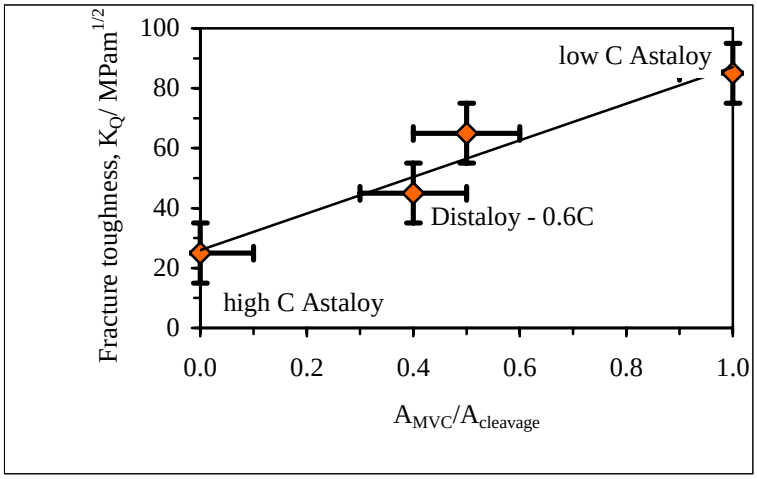

Fig.8. Apparent dependence of K_Q on the ratio of microvoid coalescence to cleavage.

Fatigue crack growth

Crack growth characteristics of all materials mirror those of wrought steels. A well defined threshold range of stress intensity ΔK_{th} th is exhibited as well as a region at higher ΔK where the Paris law $da/dN = C(\Delta K)^m$, is satisfied.

Data for growth exponents, m, are in Fig.9 and 10. To put these into a designers context, note that for conventionally wrought steels it is in the range 2 to 4. Pressed and sintered materials with relative densities, ρ_r , of about 0.9 give m in the range 10 to 18. Powder forged materials with ρ_r approaching 1.0 give m in the range 2.6 to 4.0, ie comparable with those for conventionally wrought steels. Rotary compacted materials are rather more variable; relative densities are on the whole around 0.95 but crack growth exponents range from 4.6 to 12.0.

Figure 11 shows that threshold stress intensities are generally between 5 and 15 MPa√m when R = 0.1 and reduce to between 2.7 and 5.0 MPa√m when R = 0.8. There is little discernable pattern in this data.

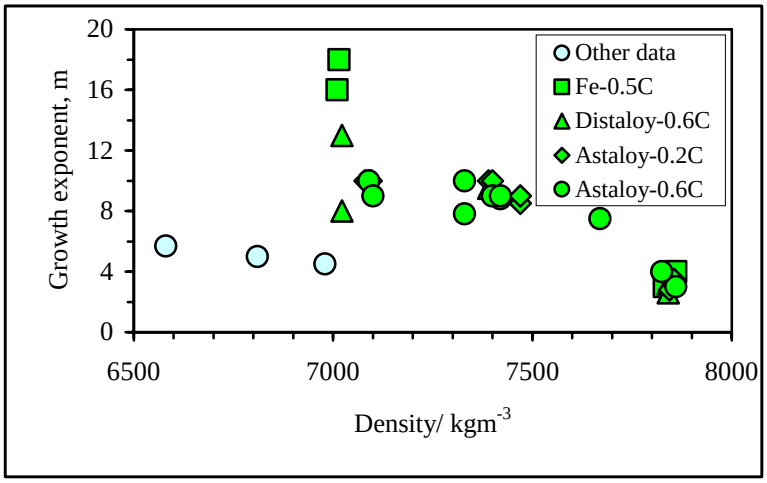

Fig.9. Paris crack growth exponents, m, as a function of density.

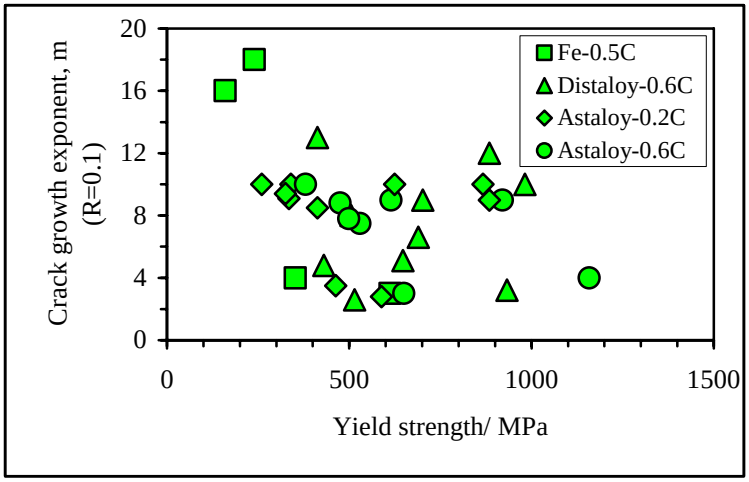

Fig.10. The relationship between yield strength and Paris crack growth exponents, m.

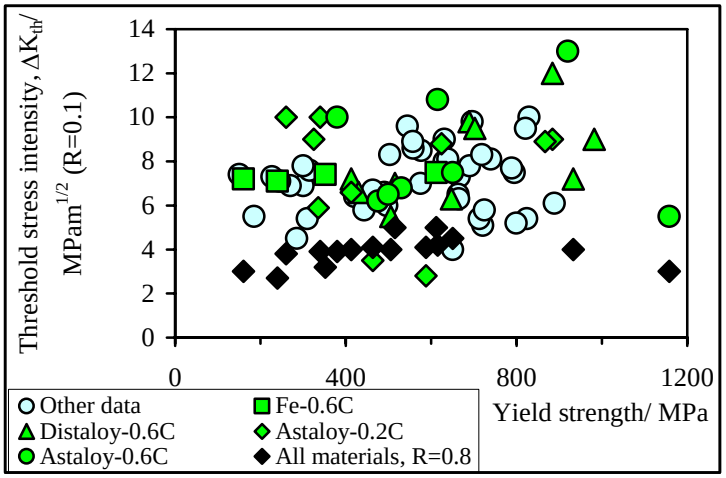

Fig.11. The interdependence of threshold stress intensities and yield strength.

Fatigue fracture surfaces

Fracture surfaces in fatigue differ according to whether they were formed at low values of ΔK just above threshold, or at high values of ΔK where K_{MAX} might be a large fraction of K_Q. Tab.3 gives a summary.

Tab.3. Summary of Fatigue Fracture Surfaces.

Material	ρ_r	Near threshold	Above threshold
Fe - 0.6%C	0.9	rpz/a~1 - 2.5, nearly planar, progressive neck failure, mix of true fatigue & MVC	rpz/a ~4 - 9, less planar, more MVC
	0.99	rpz/a < 1, flat fractures, mix of true fatigue & cleavage	rpz/a ~1 - 2, flat fractures, more cleavage
Astaloy 0.2%C	0.9	rpz/a <1, nearly planar, true fatigue & MVC, inter & trans granular	rpz/a ~2 - 4,original particles not too evident, more MVC
	0.99	rpz/a < 1, nearly planar, true fatigue, MVC & cleavage, inter & trans granular	rpz/a < 1, more cleavage
Astaloy 0.6%C	0.9	rpz/a < 1, rough surface, cracks climb & descend, some forced through particles	rpz/a<1, mainly MVC witin necks
	0.99	rpz/a <1, crack propagation through particles, lot of cleavage	rpz/a<1, grain boundary separation
Distaloy 0.6%C	0.9	rpz/a<1, nearly planar, true fatigue & MVC, inter & trans granular	rpz/a<1, original particles not too evident, more MVC
	0.99	rpz/a <1, nearly planar, true fatigue, MVC & cleavage, inter & trans granular	rpz/a < 1, more cleavage
rpz/a is the ratio of reverse plastic zone size to particle diameter			

Pressed and sintered materials subjected to high ΔK reveal large areas of apparently undeformed particles; only about 20% of the fracture surface is occupied by failed necks.

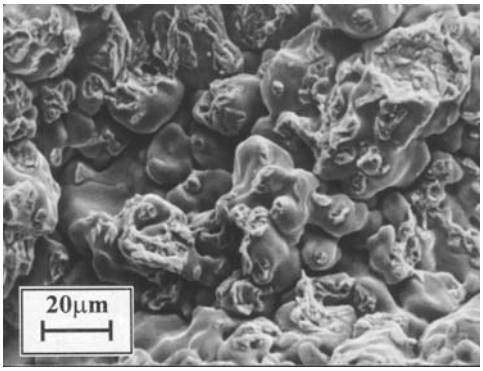

Fig.12. Fatigue fracture surface for pressed and sintered Distaloy AB – 0.6% C, ρ_r = 0.90; R = 0.1; ΔK = 11 MPa√m. K_{MAX} = 12.2 MPa√m (above threshold).

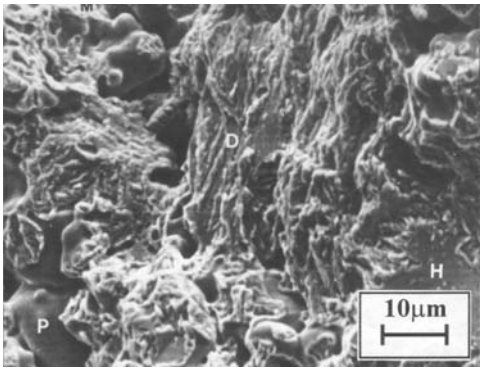

Fig.13. Fatigue fracture surface for pressed and sintered Astaloy A – 0.2% C, ρ_r = 0.90; R = 0.1; ΔK = 10 MPa√m. K_{MAX} = 11.1 MPa√m (near threshold).

Within those, microvoid coalescence is the dominant failure mode, as in Fig.12. Fractures formed at near threshold conditions are much flatter overall and failure of interparticle necks is now only partly by MVC. True transgranular fatigue modes are also found. As illustrated in Fig.13, these are not in the form of classical fatigue striations, which appear to be confined to close-packed metals, but are anisotropically textured and characteristic of those found for wrought steels. The ratio of MVC to true fatigue modes increases as ΔK is increased.

Nearly fully dense powder forgings appear to fatigue by a mixture of true fatigue modes, MVC and bursts of cleavage (Fig.14 & 15). As might be expected, the extent of cleavage increases as ΔK increases.

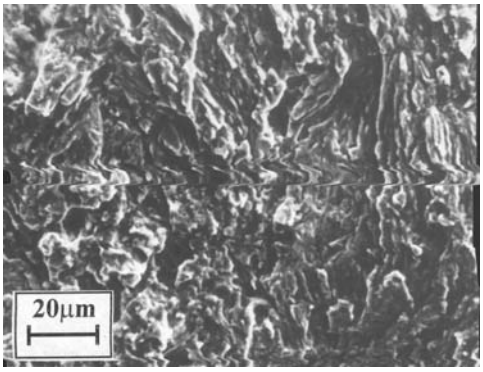

Fig.14. Fatigue fracture surface for powder forged Distaloy AB – 0.6% C, ρ_r = 0.99; R = 0.1; ΔK = 10 MPa√m. K_{MAX} = 11.1 MPa√m (near threshold).

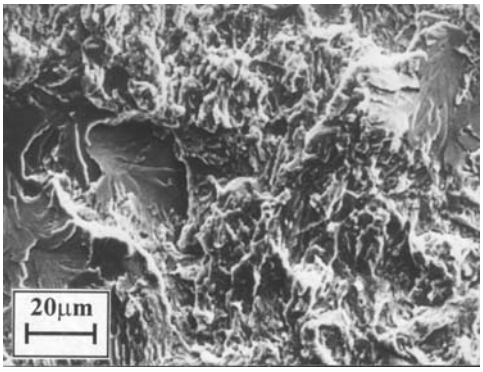

Fig.15. Fatigue fracture surface for powder forged Distaloy AB – 0.6% C, ρ_r = 0.99; R = 0.1; ΔK = 25 MPa√m. K_{MAX} = 27.8 MPa√m (Paris steady state regime).

DISCUSSION

Toughness and rates of fatigue crack growth are intimately related properties. Figure 16 shows how the Paris growth exponent relates to the fracture toughness. PM materials follow the same broad trend as wrought steels, lower values of m being associated with high toughnesses. Typically, wrought steels have values of m of less than 4. To achieve the same values for PM materials with some reliability means that toughnesses in excess of ~80 MPa$\sqrt{m}$ are required. It follows that to really get to grips with fatigue behaviour we must begin with toughness.

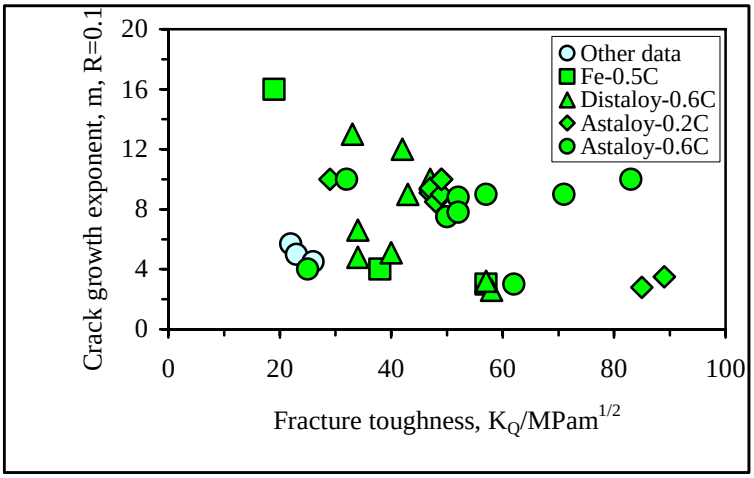

Fig.16. The significance of fracture toughness to the crack growth exponent.

Toughness

It is well established that the mechanical performance of PM materials is governed by the geometry of the continuous load bearing path within them and by the properties of those mechanical elements in that path.

In our case, when ρ_r~0.9 we have interconnected pores. The main bulks of the particles deform hardly at all and act only as transmitters of load to sinter necks; failure across a particle is a rare event. Strain is localised at the necks, which are flimsy in comparison to the particles. The necks are generally wide in relation to their thickness, even allowing for a considerable degree of uncertainty in what is meant by thickness.

The neck geometry is such that plane-strain conditions prevail within them. Rupture is most usually by the formation of microvoids after extensive local plastic flow. It is easy to see that both strength and fracture toughness should increase together as the neck diameters are increased and/or the local strength and work-hardening characteristics are improved.

Failure of sinter necks one after another often give rise to surfaces that are rough on a micro-scale. Cracks climb around particles to find the easy path. This means that the true cross-sectional area that has fractured, A_f, is not the complement of the planar porosity, A_p. A number of ideas arise from this. For example, it has been shown that the yield and maximum strengths scale with A_f and that $A_f = (1 - A_p)^{2/3}$ [19]. Overall ductilities can be thought of as determined by the local ductility of a sinter neck, diluted in the ratio of neck thickness to particle size [18].

Another approach [21] considers the work done on the material per unit volume when necks deform. The argument is that mechanical work is done only on the neck material and so the more neck material there is, the more work has to be done. A simple model leads to $V_{neck}/V_{total} \sim \rho_r N(x/a)^n$, where ρ_r is the relative density of the material, N is the co-ordination number for particles in the array (typically~10) and x/a is the ratio of sinter neck diameter to particle size. The exponent n has values between 3 and 4, depending on assumptions about how thick the neck is, and how that relates to the value of x/a. Extending the approach leads to $W_{PM}/W_{SOLID} \sim 10\rho_r (x/a)^{3.5}$ where W_{PM} is the work done per unit volume in the PM material as a whole, W_{SOLID} is that done per unit volume in the solid material occupying the sinter neck. Note the sensitivity to neck size, and of course, the importance of the material locally occupying the neck.

This approach is relevant when, as here, the plastic zone associated with an advancing crack extends to a volume that incorporates many particles. Typically, with $\rho_r \sim 0.9$ and $x/a \sim 1/3$ we have $W_{PM}/W_{SOLID} \sim 0.2$. Fracture toughnesses of pressed and sintered materials are~30 MPa$\sqrt{m}$, which may be compared with those of equivalent solid materials ~100-150 MPa$\sqrt{m}$, ie a ratio of 0.3 – 0.2. Is this just a beguiling coincidence or is it possible to deduce that the fracture toughness is directly related to the volume of material actually involved in the fracture process and the deformation that precedes it?

As the necks increase in size and become more resistant to the applied loads, the most energetically favourable path for fracture begins to move away from the necks. Some transparticle fracture now begins. This is encouraged when there is a noticeable difference between the fracture resistances of the local materials occupying the necks and the main bulks of the particles. In the case of homogeneously alloyed materials, there is little difference between compositions, microstructures and properties of the particles and the sinter necks. On the other hand, the Distaloys used here give rise to particle surfaces and neck regions that are relatively rich in nickel and other alloying elements. The Ni, in particular, encourages retention of austenite on quenching with benefits to local strength, work hardening behaviour and overall ability to absorb mechanical work before fracture. In the Distaloy used in this case, an overall 5% of the metal was measured as retained austenite. If we assume that all the retained austenite is in the sinter necks and that the necks account for about 20% of the total metal volume, that gives a local retained austenite content of ~25%. This would undoubtedly have major consequences to the local deformation and would tend to throw the path of crack advance away from the interparticle necks. Of course the argument cannot be sustained quantitatively, but something of this sort must be going on.

In nearly fully dense materials, the load bearing path is through a mathematical continuum which is interrupted by the occasional pore and inclusion. Behaviour translates directly from that of conventionally wrought materials. One difference remains. How do heterogeneous microstructures differ from homogeneous ones?

Heterogeneous microstructures offer both tough and less tough regions of the material in the path of an advancing crack. Mixed mode failures are a consequence, the overall fracture toughness being governed by the ratio of tough to cleavage modes.

Fatigue crack growth above ΔK_{th}

Crack extension in the Paris regime is partly by true fatigue modes and partly by bursts of monotonic modes. Because the applied stress intensities are lower than in monotonic loading the plastic zones at the tips of advancing cracks are smaller. Often they are of the same order as particle sizes [44]. This means that cracks are constrained to propagate in a nearly planar manner, but still try to find the easy route. Sometimes this is by

progressing through the bulk of a particle rather than by going around the periphery of it. If the plastic zone is large enough to encompass several particles, the advancing crack samples an average microstructure and failure is thrown more toward a monotonic mode. In our case, this is true of Fe-C and low C Astaloy at ρ_r~0.9 and failure, even in fatigue, is by successive failure of necks by MVC.

Distaloys and high C Astaloys are stronger and at low ΔK the plastic zones are much smaller. Cracks can advance by true fatigue modes and often climb and descend around particles in order to find the path of least resistance. At higher ΔK, plastic zones are larger and fracture surfaces reveal monotonic modes as well as true fatigue modes. In general, the proportion of a fracture surface occupied by monotonic modes increases as K_{MAX} increases toward K_{IC}. We have $A_f = (1 - A_m) = k(K_{IC} - K_{MAX})^n$, where A_f is the area fraction of the fracture surface occupied by true fatigue modes, A_m is that occupied by monotonic modes [10]. For wrought steels, n = 1. For PM materials, n ~ 1.1 when the relative density approaches unity and n ~10 when ρ_r ~ 0.9 (Fig.17).

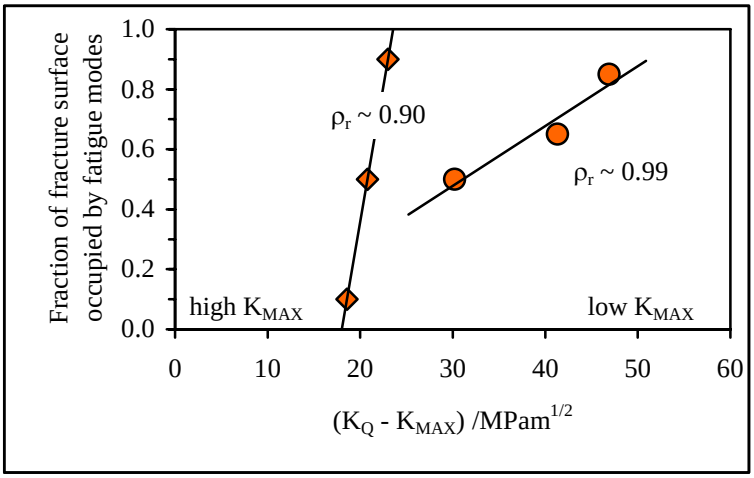

Fig.17. The fraction of fatigue fracture surfaces occupied by true fatigue modes.

Threshold stress intensities and crack growth near thresholds

When ΔK is just above ΔK_{th}, the reverse plastic zone sizes are typically <80 μm or so, ie close to the sizes of individual original particles. The exception is for Fe-C, which has zone sizes of the order of 2 or 3 particles. Small reverse plastic zones mean that fewer contact necks are contained within a plastic zone and a crack propagates from neck to neck in such a way as to maintain an overall flat fracture surface.

Calculated crack opening displacements, $\delta_{max} = 0.245(K_{max}^2/\sigma_y E)$, are small, generally less than 2-4μm [44]. Interactions between asperities on opposing faces of the fracture are likely and roughness induced crack closure effects come into play. Inability of the crack to close properly means that the crack tip is shielded from the full range of ΔK and K_{min} does not relax back to its proper value. This is an acknowledged recipe for increasing the value of the threshold, ΔK_{th}.

Increasing the R-ratio from 0.1 to 0.8 means that both K_{max} and K_{min} are increased (at the same ΔK). Crack closure effects are reduced, the crack tip sees what is applied

without being shielded and there is a reduction in ΔK_{th}. Thresholds at R = 0.8 are consistently lower than those at R-0.1, by between ~1.5 and 6.5 MPa√m.

CONCLUSIONS

When ρ_r<0.9, toughness and strength are both governed by the proportion of the overall material that is actually used to absorb strain energy in the sinter necks between particles. This proportion scales with $(x/a)^n$, where n is ~3 – 4. In other words, it is very sensitive to the sintering parameters that decide x/a.

Both strength and toughness are also affected by the local strengths, ductilities and work-hardening characteristics of the necks, which in turn are functions of their local composition and microstructure. Local accumulations of those elements which help to retain austenite are thought to be beneficial.

When ρ_r>0.95 and approaches 1.0, relationships between toughness and strength are similar to those for wrought steels, toughness generally diminishing as strength increases. Fracture modes can be by microvoid coalescence, by cleavage, or by a mixture of the two. The larger the amount of MVC, the tougher the material.

Fatigue crack growth rates in PM steels follow the general trends with K expected from wrought steels.

Threshold stress intensities are between 5.5 and 11 MPa√m when R = 0.1 and between 2.7 and 5.0 MPa√m when R = 0.8. The large reductions in Kth brought about by increasing R are evidence for roughness induced closure effects.

Paris exponents are between 8 and 18 when the porosity is ~10% but between 2.5 and 4.0 at near full density. Wrought steels usually have Paris exponents of ~2-4.

Fatigue behaviour is intimately bound up with toughness. To achieve fatigue growth exponents comparable with those of wrought steels requires fracture toughnesses of more than about 80 MPa√m or better.

Fracture processes in fatigue are affected both by porosity and by the basic strength and toughness of the material. At 10% porosity, Fe-C fails mostly by progressive rupture of sinter necks, almost exclusively by microvoid coalescence. Other materials have smaller reverse plastic zone sizes and the cracks are constrained to behave more like conventional fatigue cracks. They propagate by mixtures of true fatigue modes and monotonic modes depending on how close the maximum applied stress intensity approaches the fracture toughness, KIC.

ACKNOWLEDGEMENTS

It is a pleasure to acknowledge all those friends and colleagues over the years with whom I have shared the adventures of finding things out. In particular, Drs Julia King, now at Rolls-Royce and Dick Leheup, now dead, have taught me much and put up with my mistakes with good humour. I owe them a great deal.

REFERENCES

[1] Williams, B., Albano-Muller, L.: In: DFPM 1996, Deformation and Fracture in Structural Materials, High Tatras, 1996. Kosice : IMR SAS, 1996, vol. 1, p. 17
[2] Parilak, L., Danninger, H.: DFPM 1999, Deformation and Fracture in Structural Materials, Piestany, 1996. Kosice : IMR SAS, 1999
[3] Esper, FJ., Sonsino, CM.: Fatigue design for PM components. Shrewsbury : EPMA, 1994
[4] Sonsino, CM.: In: PM2001 European Congress and Exhibition on Powder Metallurgy, Nice, 2001. Shrewsbury : EPMA, 2001, vol. 2, p. 80

[5] Knott, JF.: Fatigue crack growth: 30 years of progress. London : Pergamon Press, 1973
[6] O'Brien, RC.: Metal Powder Report, vol. 43, 1988, p. 744
[7] James, W., O'Brien, RC.: Metal Powder Report, vol. 42, 1987, p. 250
[8] Williams, SH., Haynes, R.: Powder Metallurgy, vol. 16, 1973, p. 387
[9] Danninger, H., Weiss, B.: Powder Metallurgy Progress, vol. 1, 2001, p. 19
[10] Mosca, E.: Guide to the design of sintered parts. Torino : ASSINTER, 1996
[11] Dalgic, M., Beiss, P.: In: Materials Development and Processing. Proc. EUROMAT'99, vol. 8. Eds. L. Schultz, D.M. Herlach, J.V. Wood. Weinheim : Wiley-VCH, 2000
[12] Leheup, ER., Moon, JR.: Powder Metallurgy, vol. 21, 1978, p. 1
[13] Kulcinski, G., Wagner, P., Cowder, LR.: Journal Less Common Metals, vol. 17, 1964, p. 390
[14] Moon, JR.: Powder Metallurgy, vol. 32, 1989, p. 132
[15] Jandeska, WF.: Metal Powder Report, vol. 40, 1985, p. 90
[16] Tengzelius, J.: Metal Powder Report, vol. 43, 1988, p. 757
[17] Salak, A., Miskovic, V., Dudrova, E., Rudnayova, E.: Powder Metallurgy International, vol. 6, 1974, p. 128
[18] Slesar, M., Dudrova, E., Parilak, L., Pelikan, K.: Powder Metallurgy International, vol. 19, 1987, p. 23
[19] Slesar, M.: In: DFPM 1996, Deformation and Fracture in Structural Materials, High Tatras, 1996. Kosice : IMR SAS, 1996, vol. 1, p. 85
[20] Moon, JR. In: DFPM 1996, Deformation and Fracture in Structural Materials, High Tatras, 1996. Kosice : IMR SAS, 1996, vol. 1, p. 61
[21] Moon, JR.: In: DFPM 1999, Deformation and Fracture in Structural Materials, Piestany, 1999. Kosice : IMR SAS, 1999, vol. 1, p. 214
[22] Brown, GT., Steed, JA.: Powder Metallurgy, vol. 16, 1973, p. 405
[23] Steed, JA.: Powder Metallurgy, vol. 18, 1975, p. 201
[24] Dogan, B., Davies, TJ.: Powder Metallurgy International, vol. 15, 1983, p. 11
[25] Beiss, P.: Metal Powder Report, vol. 42, 1987, p. 243
[26] Mellanby, IJ., Moon, JR., Leheup, ER.: Powder Metallurgy, vol. 30, 1987, p. 125
[27] Mellanby, IJ., Moon, JR.: Modern Developments Powder Metallurgy, vol. 18, 1988, p. 183
[28] Douib, N., Mellanby, IR., Moon, JR.: Powder Metallurgy, vol. 32, 1989, p. 209
[29] Danninger, H. In: DFPM 1996, Deformation and Fracture in Structural Materials, High Tatras, 1996. Kosice : IMR SAS, 1996, vol. 1, p. 27
[30] Knott, JF. In: Advances in the physical metallurgy and applications of steels. London : The Metals Society, 1982
[31] Ashby, MF.: Materials selection in mechanical design. Oxford : Butterworth – Heinemann, 1999
[32] Barnby, JT., Ghosh, G., Dinsdale, K.: Powder Metallurgy, vol. 16, 1973, p. 55
[33] Fleck, NA., Smith, RA.: Powder Metallurgy, vol. 24, 1981, p. 121
[34] Bastian, FK., Charles, JA.: Powder Metallurgy, vol. 21, 1978, p. 199
[35] Crane, LW., Farrow, RJ.: Powder Metallurgy, vol. 23, 1980, p. 198
[36] Saritas, S., James, WB., Davies, TJ.: Powder Metallurgy, vol. 24, 1981, p. 131
[37] Phillips, RA., King, JE., Moon, JR.: Powder Metallurgy, vol. 43, 2000, p. 43
[38] Dudrova, E., Parilak, L., Kabatova, M., Danninger, H.: In: DFPM'99, Deformation and fracture of structural PM materials, Piestany, 1999. Kosice : IMR SAS, 1999, vol. 1, p. 250
[39] Navarra, E., Bengtsson, B.: International Journal Powder Metallurgy and Technology,

vol. 20, 1984, p. 33
[40] Peacock, S., Moon, JR.: Powder Metallurgy, vol. 43, 2000, p. 49
[41] Bertilsson, L., Karlsson, B.: Powder Metallurgy, vol. 30, 1987, p. 183
[42] Sonsino, CM., Schlieper, G., Huppman, WJ.: International Journal Powder Metallurgy, vol. 20, 1984, p. 45
[43] Lindner, KH., Sonsino, CM. In: PM 94 World Congress Powder Metallurgy, 1994, Les Ulis, Les Editions de Physique.
[44] Phillips, RA., King, JE, and Moon, JR.: Powder Metallurgy, vol. 43, 2000, p. 149
[45] Peacock, S., Moon, JR.: Powder Metallurgy, vol. 43, 2000, p. 345
[46] Standring, PM., Moon, JR.: Powder Metallurgy, vol. 35, 1992, p. 193
[47] Kapp, JA., Newman Jr, JC, Underwood, JH.: Journal of testing and evaluation, vol. 8, 1980, p. 314